Materials Science, Vol. 20, No. 1, 2002

Effects of polarization of radiofrequency radiation in polycrystalline ESR

V.E. FAINZILBERG

Department of Chemistry, Long Island University, USA

ESR spectrum of polycrystalline samples exposed to radiofrequency radiation of circular polarization is calculated and examined. The spectrum is compared with ESR spectrum generated by commonly used oscillating magnetic field of linear polarization. Differences of contours at linear and circular polarizations provide additional opportunity for correlation of theory and experiment, and determination of ESR parameters.

Key words: ESR spectrum, polycrystalline samples, circular polarization

1. Introduction

Radiofrequency radiation, commonly used in ESR experiments, is linearly polarized. Utilization of a circular-polarized radiofrequency radiation is essential in some cases, when the sign of gyromagnetic ratio may reveal the nature of the ground state. It permits also to determine the signs of **g**-tensor components in the systems with ground state described as an effective spin level [1–3]. Multiple experiments and calculations of line shapes of mono- and polycrystalline ESR spectra have exclusively been carried out with linear-polarized radiation (see, e.g., [4–8]). Indeed, any linear-polarized radiation is a superposition of two circular components that revolve in opposite directions, and hence, while one of them may be silent, the other one is absorbed. We aim to show that polycrystalline spectrum in linear-polarized radiation has different line shape than that obtained in a circular polarization. The latter provides additional data to compare and validate theoretical models. In this paper, the theory of polycrystalline ESR spectra that are generated by a resonance absorption of a circularly polarized radiofrequency radiation are examined.

2. Transition operator of a circularly polarized radiation

Operator of Zeeman interaction of a paramagnetic center (effective spin, **s**) with an oscillating magnetic field **B** is written as [1–5]:

PDF created with FinePrint pdfFactory trial version http://www.fineprint.com

$$\mathbf{V} = -b\mathbf{s}g\mathbf{B}$$

where b and g are Bohr's magneton and **g**-tensor, respectively (here and further a circumflex above letter indicates the operator and/or tensor). Omitting constant multiplier $b\mathbf{B}$ we obtain the transition operator in the form of:

$$\hat{V} = \hat{s}^{\dagger}\,\hat{\mathrm{g}}\,\mathbf{e} \qquad (1)$$

where polarization vector $\mathbf{e} = \tilde{\mathbf{B}}/\tilde{B}$ defines the orientation of an oscillating magnetic field.

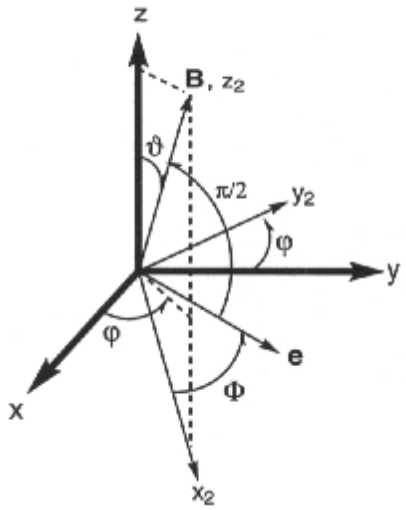

Fig. 1. Orientation of external constant magnetic field **B** and polarization vector **e** of oscillating magnetic field in the co-ordinate system, *x*, *y*, *z* of an individual arama netic center

Usually, in ESR spectrometers, the oscillating magnetic field (either linear-, or circular-polarized) is localized in the plane perpendicular to the external constant magnetic field **B**.

Consider system *x*, *y*, *z* of an individual paramagnetic center (Fig. 1). The orientation of the external field **B** is chosen along z_2-axis, while x_2y_2-plane accommodates the polarization vector **e** of the oscillating radiation. Co-ordinate system $x_2y_2z_2$ can be obtained from the system of an individual center *xyz* by two successive rotations, namely: (1) right-handed rotation around *z*-axis by an angle j to obtain intermediate system, $x_iy_i(z_i \equiv z)$:

$$\begin{pmatrix} x_1 \\ y_1 \\ z_1 \end{pmatrix} = \hat{u} \cdot \begin{pmatrix} x \\ y \\ z \end{pmatrix} \equiv \begin{pmatrix} \cos j & \sin j & 0 \\ \sin j & \cos j & 0 \\ 0 & 0 & 1 \end{pmatrix} \cdot \begin{pmatrix} x \\ y \\ z \end{pmatrix}$$

followed by (2) right-handed rotation around newly formed y_1-axis by an angle J :

PDF created with FinePrint pdfFactory trial version http://www.fineprint.com

$$\begin{pmatrix} x_2 \\ y_2 \\ z_2 \end{pmatrix} = \hat{u}_J \cdot \begin{pmatrix} x_1 \\ y_1 \\ z_1 \end{pmatrix} \equiv \begin{pmatrix} \cos J & 0 & -\sin J \\ 0 & 1 & 0 \\ \sin J & 0 & \cos J \end{pmatrix} \cdot \begin{pmatrix} x_1 \\ y_1 \\ z_1 \end{pmatrix}$$

where x_j, y_j, and z_j assume components of an arbitrary vector written in each of coordinate systems. The relationship between components of the vector in two coordinate systems is given by [9, 10]:

$$\begin{pmatrix} x_2 \\ y_2 \\ z_2 \end{pmatrix} = \hat{u} \cdot \begin{pmatrix} x \\ y \\ z \end{pmatrix}$$

where

$$\hat{u} = \hat{u}_J \cdot \hat{u}_j \equiv \begin{pmatrix} \cos J \cos j & \cos J \sin j & \sin J \\ -\sin j & \cos j & 0 \\ \sin J \cos j & \sin J \sin j & \cos J \end{pmatrix} \tag{2}$$

The immediate orientation of polarization vector **e** in the system, x_2, y_2, z_2 is defined as (see Fig. 1).:

$$e_{x_2} = \frac{\tilde{\tilde{B}}_{x_2}}{\tilde{\tilde{B}}} \equiv \cos \Phi, \quad e_{y_2} = \frac{\tilde{\tilde{B}}_{y_2}}{\tilde{\tilde{B}}} \equiv \sin \Phi, \text{ and } e_{z_2} = \frac{\tilde{\tilde{B}}_{z_2}}{\tilde{\tilde{B}}} \equiv 0$$

Thus, the polarization vector in the *x*, *y*, *z*-system is obtained as

$$(0 \le J \le \pi, \quad 0 \le j \le 2\pi, \quad 0 \le \Phi \le 2\pi):$$

$$\begin{pmatrix} e_x \\ e_y \\ e_z \end{pmatrix} = \hat{u}^{-1} \cdot \begin{pmatrix} \cos \Phi \\ \sin \varphi \\ 0 \end{pmatrix}, \quad \Leftrightarrow \quad \begin{cases} e_x = \cos J \cos j \cos \Phi - \sin j \sin \Phi \\ e_x = \cos J \sin j \cos \Phi - \cos j \sin \Phi \\ e_x = -\sin J \cos \Phi \end{cases} \tag{3}$$

In the case of axial anisotropy the **g**-tensor is diagonal with: $g_{xx} = g_{yy} \equiv g_\perp$ and $g_{zz} \equiv g_\parallel$. In the cyclic basis [11, 12], $x_0 = z$, $x_\pm = \mathbb{m} \, 1/\sqrt{2} \, (x \pm iy)$, the transition operator has a simple form, and in the case of a linear polarization we obtain the a well-known expression [13]:

PDF created with FinePrint pdfFactory trial version http://www.fineprint.com

$$\begin{aligned}\hat{V}_{\text{lin}} &= -g_{\|}e_0\hat{s}_0 + g_{\perp}(e_+\hat{s}_- + e_-\hat{s}_+) \\ &\equiv g_{\|}\sin J\cos\Phi\hat{s}_0 + \tfrac{1}{\sqrt{2}}g_{\perp}\Big[(\cos J\cos\Phi - i\sin\Phi)e^{-ij}\,\hat{s}_+ \\ &-(\cos J\cos\Phi + i\sin\Phi)e^{ij}\,\hat{s}_-\Big]\end{aligned} \tag{4}$$

where $\hat{s}_+$ and $\hat{s}_-$ are commonly known raising and lowering spin operators, respectively.

General case of an elliptically-polarized radiation [15, 16] is given by a complex polarization vector: $\mathbf{e} = \mathbf{e}_1 \pm i\mathbf{e}_2$. In a particular case of $|\mathbf{e}_1| = |\mathbf{e}_2|$, and $\mathbf{e}_1 \perp \mathbf{e}_2$, elliptically-polarized radiation is reduced to a right-handed: $\mathbf{e}_+ = \mathbf{e}_x + i\mathbf{e}_y$, and left-handed: $\mathbf{e}_- = \mathbf{e}_x - i\mathbf{e}_y$, circular-polarized radiations. Hence, the transition operator of interaction with a circular-polarized oscillating field related to x_2, y_2, z_2-system is given by:

$$\hat{V}_{\text{cir}}^{\pm} = \hat{m}_{\mathbf{m}}e_{\pm} \equiv -m_{\mathbf{m}}e^{\pm i\Phi} \equiv -\tfrac{1}{\sqrt{2}}(\hat{m}_{x_2} \pm i\hat{m}_{y_2})e^{\pm i\Phi}, \tag{5a}$$

where upper + and lower – superscripts (subscripts) correspond to the right-handed, and left-handed circular-polarized radiofrequency radiations, respectively. Applying unitary transformation (3) to (5a) we can rewrite the right-handed circular-polarized transition operator in the system, x, y, z, of individual center in the form of:

$$V_{\text{cir}} = \left\{\frac{1}{\sqrt{2}}g_{\|}\sin J\hat{s}_0 + \frac{1}{2}g_{\perp}\Big[(\cos J - 1))e^{-ij}\,\hat{s}_+)(\cos J + 1)e^{ij}\,\hat{s}_-\Big]\right\}e^{i\Phi} \tag{5b}$$

Transition operator (4) for a linear polarization can be also expressed as a superposition of clockwise- and counterclockwise circular polarizations:

$$\hat{V}_{\text{lin}} = \frac{1}{\sqrt{2}}(\hat{V}_{\text{cir}}^{+} + \hat{V}_{\text{cir}}^{-})$$

3. Calculation of line shapes of polycrystalline samples

We consider first the polarization effects in ESR of an isolated Kramers doublet with an axial anisotropy of g-factors. Zeeman interaction is described by a standard spin Hamiltonian:

$$\hat{H}_Z = -\hat{\mu}B \equiv -\left[g_{\|}\cos J\hat{s}_0 + \frac{1}{\sqrt{2}}g_{\perp}\sin J\left(e^{ij}\,\hat{s}_- - e^{-ij}\,\hat{s}_+\right)\right]\beta B \tag{6}$$

PDF created with FinePrint pdfFactory trial version http://www.fineprint.com

with the energies (s = ½): $E_{\pm} = \pm\frac{1}{2} g(J)\, bB,$ where

$$g(J) = \sqrt{g_{\parallel}^2 \cos^2 J + g_{\perp}^2 \sin^2 J}$$

Integral ESR contours of powder spectrum are generated by:

$$J_k(B) = \frac{1}{8\pi^2} \int_0^{\pi} \sin J\, dJ \int_0^{2\pi} dj \int_0^{2\pi} W_k(J, \Phi)\, r(J, B, e)\, dF \tag{7}$$

where $\varepsilon = h\nu$ is radiofrequency quantum; $W_k(J, F)$ is the probability of a transition at a given polarization κ (either linear, or circular), and $r(J, B, e)$ is the form-function of absorption of an individual paramagnetic center. In the case of Kramers doublets the spectrum is generated by the only transition: $W_k(J, F) = \left| \left\langle E_+ \left| \hat{V}_k \right| E_- \right\rangle \right|,$ and in linear polarized radiation the latter takes the form [1–3]:

$$W_{\text{lin}} = \frac{1}{4} g_{\perp}^2 b^2 \left[\frac{g_{\parallel}^2}{g^2(J)} \cos^2 F + \sin^2 F \right] \tag{8}$$

Using the operator (5b) we obtain the transition probability in the case of a circular-polarized radiation as:

$$W_{\text{cir}}^{\pm} = \frac{1}{8} g_{\perp}^2 b^2 \left[\frac{g_{\parallel}}{g(J)} \pm 1 \right]^2 \tag{9}$$

Both probabilities depend on the angles h and M, which define the orientation of polarization vector **e** in the plane perpendicular to the external field **B.** This dependence vanishes only in a canonical orientation of the external magnetic field, h = 0. In this particular case the standard relation $W_{\text{cir}}^{\pm}/W_{\text{lin}}$ = 2, applies that is peculiar for relation, '~'lin the axial symmetry. We would like to stress that this result is not related to a relative amplification of a spectrometer, and is obtained under the assumption of the same amplitude of radiofrequency radiation and, hence, of the same rates of radiofrequency energy that enters the absorption center in both circular and linear polarizations. In arbitrary ($h \neq 0$) field, the ratio, $W_{\text{cir}}^{\pm}/W_{\text{lin}}$ is no longer equal to 2 and is substituted by a more complicated expression that follows from formulas (8) and (9). In addition, more complicated systems (that involve spin-orbital contributions to effective spin levels [13]) bring also the field dependence into expressions of probabilities and their ratios.

PDF created with FinePrint pdfFactory trial version http://www.fineprint.com

We consider next the simplest theoretical model without broadening of individual absorption with form-function, $r(J,B,e)=d\left[g(J)bB-e\right]$. Using Eqs. (7) and (9), we arrive at the following contours of ESR lines of polycrystals in the case of circular-polarized radiation (Fig. 2, $g_{\|} > g_{\perp}$ is assumed here):

$$J_{\text{cir}}^{\pm}(B)=\frac{g_{\perp}^{2}b\left(e\pm g_{\|}bB\right)^{2}}{8eB\left(g_{\|}^{2}-g_{\perp}^{2}\right)\left(e^{2}-g_{\perp}^{2}b^{2}B^{2}\right)} \tag{10}$$

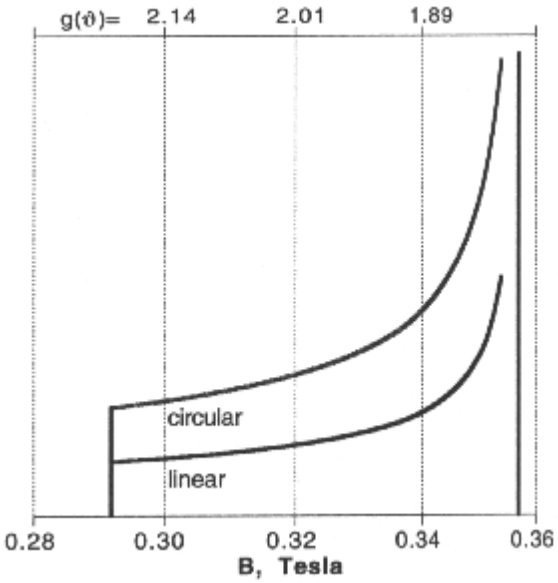

Fig. 2. Line shapes of polycrystalline ESR in the right-handed circular and linear polarizations of quantum, ε = 9 GHz ≡ 0.3 cm^{-1}, for $g_{\|}$ = 2.2, $g_{\perp}$= 1.8

Same calculations carried out using Eqs. (7) and (8) yield well-known expression for the contours [1–3] referred to absorption of a linear-polarized radiation (Fig.2):

$$J_{\text{lin}}(B)=\frac{g_{\perp}^{2}b\left(e^{2}\pm g_{\|}^{2}b^{2}B^{2}\right)}{8eB\left(g_{\|}^{2}-g_{\perp}^{2}\right)\left(e^{2}-g_{\perp}^{2}b^{2}B^{2}\right)} \tag{11}$$

Comparison of these results exhibits a simple ratio of intensities corresponding to the circular and linear polarizations:

$$J_{\text{cir}}^{\pm}(B)=\frac{\left(e\pm g_{\|}bB\right)^{2}}{e^{2}+\left(g_{\|}bB\right)^{2}} \tag{12}$$

PDF created with FinePrint pdfFactory trial version http://www.fineprint.com

Thus, the line shape in a circular polarization is characterized by a similar square root divergence as in the case of a linear-polarized absorption in the field perpendicular to the axial axis. In the field parallel to the axial *z*-axis, the intensity of the right-handed circular-polarized absorption is twice of that at a linear-polarized radiation in agreement with the above consideration. The ratio of intensities slowly decreases with the increasing field while moving towards the right-hand side of the contour (Fig. 2).

Equation (12) allows one to determine the value of the parallel *g*-factor, $g_{\parallel}$. With proper fitting of theoretical and experimentally observed contours in the two polarizations, followed by comparison of one, or several points of the line contours, Eq. (12) provides additional possibility and greater accuracy of parameter's evaluation. Similar approach can be applied to differential contours, as well. The ratio of differential intensities in different polarizations is obtained as:

$$\frac{d\left(J_{\text{cir}}^{\pm}(B)\right)}{d\left(J_{\text{lin}}(B)\right)} = \frac{2\left(g_{\perp} bB\right)^2 \left(e \pm g_{\parallel} bB\right) - e\left[e^2 - \left(g_{\parallel} bB\right)^2\right]}{2\left(g_{\perp} bB\right)^2 e - e\left[e^2 - \left(g_{\parallel} bB\right)^2\right]} \tag{13}$$

Let us emphasize that the ratio of intensities of differential contours, $d[J_{\text{cir}}^{+}(e/g_{\parallel}b)]/d[J_{\text{lin}}(e/g_{\parallel}b)] = 2$, in the field parallel to the *z*-axis at right-handed circular and linear polarizations remains the same as that for the integral contours.

Formulas (12) and (13) reveal an essential practical advantage of ESR experiments using powder samples subjected to radiation in the two polarizations. Relatively simple expression (13) offers the possibility of experimental determination of both (parallel and perpendicular) *g*-factors based on the comparison of differential contours obtained in the linear and right-handed circular polarizations of radiofrequency field.

Of course, there are relaxation and other processes which cause the line broadening in real systems. Accounting for broadening of individual absorption γ brings some erosion of the edges of powder ESR line contours and makes it difficult to determine accurately the *g*-factors on the borders of the spectrum. Nevertheless, at relatively small γ (compared to orientation broadening of the spectrum), the line contours undergo only small changes in the region distant from the borders.

Consequently, Eqs. (12) and (13) represent an appropriate approximation for the central parts of real spectra.

Consider more realistic model that phenomenologically accounts for the line broadening of individual centers. We assume here the Lorentz form-function [1, 3] (with the broadening parameter γ):

$$r(J, B, e) = \frac{1}{\pi} \cdot \frac{g}{g^2 + \left[g(J) bB - e\right]^2} \tag{14}$$

Applying again Eqs. (7)–(9) we obtain the following expressions for the line contours in circular and linear polarizations (assuming $g_{\parallel} > g_{\perp}$):

PDF created with FinePrint pdfFactory trial version http://www.fineprint.com

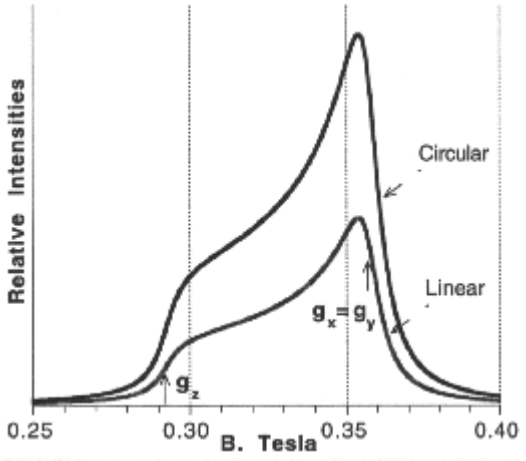

Fig. 3. Integral contours of ESR spectrum generated using Eq.(15) at g = 50 Gs ≡ 0.05 T in right-handed circular and linear polarizations of radiofrequency quantum, e = 9 GHz ≡ 0.3 cm^{-1}, at $g_{\|}$ = 2.2, $g_{\perp}$ = 1.8

$$J_{\text{cir(lin)}}(B) = \frac{g(g_{\perp}b)^2 q(g_{\|}-g_{\perp})}{4pH_{\perp}(a_{+}+a_{-})(e^2+g^2)\sqrt{h^2-1}}$$

$$\times\left\{\frac{\left(e^2+g^2-H_{\|}^2\right)\cdot a_{-}+\left(e^2+g^2\right)^2-f_{\text{cir(lin)}}(B)}{\sqrt{2a_{-}+4e^2}}\right.$$

$$\times\ln\sqrt{\frac{\left(a_{-}+2eH_{\|}\right)-H_{\perp}\sqrt{\left(2a_{-}+4e^2\right)\left(h^2-1\right)}}{\left(a_{-}+2eH_{\|}\right)+H_{\perp}\sqrt{\left(2a_{-}+4e^2\right)\left(h^2-1\right)}}}$$

$$+\frac{\left(e^2+g^2-H_{\|}^2\right)\cdot a_{+}-\left(e^2+g^2\right)^2+f_{\text{cir(lin)}}(B)}{\sqrt{2a_{+}+4e^2}}$$

$$\left.\times\left[\frac{p}{2}-\arctan\left(\frac{a_{+}-2eH_{\|}}{H_{\perp}\sqrt{\left(2a_{+}-4e^2\right)\left(h^2-1\right)}}\right)\right]\right\} \qquad (15)$$

where

$$h \equiv \frac{g_{\|}}{g_{\perp}} > 1,\ H_{\|} \equiv g_{\|}bB,\ H_{\perp} = g_{\perp}bB$$

PDF created with FinePrint pdfFactory trial version http://www.fineprint.com

and

$$\begin{cases} a\pm = \sqrt{\left(e^2+g^2+H_\perp^2\right)^2-\left(2eH_\perp\right)^2} \pm \left(e^2+g^2+H_\perp^2\right) \\ f_{\text{cir}}^{\pm}(B) = \left(e^2+g^2\pm 2eH_\parallel\right)^2 \\ f_{\text{lin}}(B) = \left(e^2+g^2\right)^2+\left(2eH_\parallel\right)^2 \end{cases} \tag{16}$$

ESR line contours in the two polarizations calculated using Eq. (15) are shown in Fig. 3. Analytical formulas (15) and (16) can be employed to determine the *g*-factor values and Lorentz broadening parameter *y*, based on the comparison of the line contours obtained in different polarizations. Differences of contours in linear and circular polarizations provide the additional possibility for correlation of theory and experiment.

Acknowledgment

Author appreciates the discussion of the subject with Yu. Rosenfeld and is extremely grateful to B.S. Tsukerblat for the review and valuable comments.

References

[1] ABRAGAM A., BLEANEY B., *Electron Paramagnetic Resonance of Transition Ions*, Vol. 1, 1970, Oxford, Clarendon Press.
[2] PAKE G.E., *Paramagnetic Resonance*, 1962, W.A. Benjamin Inc., New York.
[3] SLICHTER C.P., *Principles of Magnetic Resonance*, 2nd Ed., 1980, Springer-Verlag.
[4] TAYLOR P.C., BAUGHER J.F., KRIZ H.M., Chem. Rev., 1975, 75 (2), 203−240.
[5] JIDOMIROV L.M., LEBEDEV Ya.C., DOBRYAKOV S.N., STEINSHNEIDER N.Ya., CHIRKOV A.K., GUBANOV V.A., *Interpretation of Complex EPR Spectra* (in Russian), 1975, Moskow, Nauka.
[6] TSUKERBLAT B.S., BELINSKII M.I., FAINZILBERG V.E., Sov. Sci. Rev., 1990, 9, 339.
[7] TSUKERBLAT B.S., BELINSKII M.I. , *Magnetochemistry and Radiospectroscopy of Exchange Clusters* (in Russian), 1983, Kishinev, Shtiintza, p. 300.
[8] TSUKERBLAT B.S., *Group Theory in Chemistry and Spectroscopy.* 1994, Academic Press, p. 430.
[9] MCCLUNG R.E.D., Canadian J. Phys., 1968, 46, 2271.
[10] RUDONICZ C., J. Mag. Res., 1985, 63, 95.
[11] VARSHALOVICH D.A., MOSKALEV A.N., HERSONSKII V.K., *Quantum Theory of Angular Momentum* (in Russian), 1975, Nauka, p. 433.
[12] BIEDENHARN L.C., LOUCK J.D., *Angular Momentum in Quantum Physics*, Vol. 1, 1981, Addison-Wesley.
[13] GATTESCHI D., TSUKERBLAT B.S., FAINZILBERG V.E., Appl. Magn. Res., 1996, 10, 217−249.
[14] FAINZILBERG V.E., BELINSKII M.I., TSUKERBLAT B.S., Mol. Phys., 1981, 44, 1195−1213.
[15] LANDAU L.D., Lifshitz E.M., *Field Theory* (in Russian), 1973, Mir, p. 502.
[16] LOUDON R., *The Quantum Theory of Light*, 1973, Oxford, Clarendon Press.

PDF created with FinePrint pdfFactory trial version http://www.fineprint.com